Near-field Raman scattering investigation of tip effects on C_{60} molecules

Prabhat Verma,[1,*] Kohei Yamada,[1] Hiroyuki Watanabe,[2] Yasushi Inouye,[3,4] and Satoshi Kawata[1,4]
[1]*Department of Applied Physics, Osaka University, Osaka 565-0871, Japan*
[2]*Analysis Technology Center, Advanced Core Technology Laboratories, Fuji Photo Film Co., Ltd., Kanagawa 250-0193, Japan*
[3]*Graduate School of Frontier Biosciences, Osaka University, Osaka 565-0871, Japan*
[4]*RIKEN, Saitama 351-0198, Japan*
(Received 11 October 2005; revised manuscript received 28 November 2005; published 17 January 2006)

Near-field Raman scattering has been utilized to study the interaction between an apertureless metal coated sharp tip and C_{60} molecules. Through local plasmon polaritons generated at the metallized tip, the tip interacts electromagnetically and chemically with the sample molecules, providing an enhanced scattering and high spatial resolution beyond the diffraction limits of the probing light. An additional enhancement was observed under the gap-mode configuration. The sample molecules were uniaxially pressurized by the tip, and a mechanical interaction between the tip and the sample molecules was also investigated. The photopolymerization of C_{60} molecules was found to accelerate under the high pressure.

DOI: 10.1103/PhysRevB.73.045416 PACS number(s): 68.37.Uv, 78.30.Na

I. INTRODUCTION

The well-known diffraction limits in the conventional optical microscopy that restricts the spatial resolution to a size comparable to the half of the probing wavelength can be overcome by the near-field scanning optical microscopy (NSOM).[1–8] The NSOM technique utilizes either an aperture[1–3] or apertureless[4–8] tip to overcome the diffraction limits. Apertureless tips have a much higher resolution potential compared to the aperture tips. If an apertureless tip is metallic[6–8] and is illuminated with light, then along with a high resolution, it also generates local surface plasmon polaritons (SPPs) at the tip apex, providing an evanescent field in close proximity of the tip apex. If a sample is placed in this evanescent field, the scattering from the sample can be enhanced. The fact that light scattering can be enhanced when a sample is placed near a rough metallic surface was recognized long ago in the surface-enhanced Raman scattering (SERS).[9–12] While SERS can enhance the scattering, it cannot provide significantly high resolution. However, when Raman scattering is combined with NSOM technology, known as the tip-enhanced Raman scattering (TERS), it can provide both enhancement as well as high spatial resolution much below the diffraction limits of the probing light.[13–17] Ideally, it is possible to achieve molecular resolution with this technology. After the invention of the apertureless tip, TERS has been widely utilized by our group[13–17] as well as other researchers[18–20] to study several samples, including the nanomaterials, such as carbon nanotubes and DNA structures.

It is usually understood that the tip interacts with the sample molecules immersed in the evanescent field in two different ways—electromagnetically and chemically. In addition, we investigated the mechanical interaction between the tip and the sample. Local SPPs at the surface of a small metal structure can be excited by light irradiation, if the metal size is much smaller than the wavelength of the light. These excited SPPs interact back with the electromagnetic field of the light and the electromagnetic field in the vicinity of the metal structure is greatly enhanced. The amplification of both the incident laser field and the Raman scattered light field through their interaction with the surface constitutes the electromagnetic mechanism of field enhancement. Since this enhanced field is extremely localized at the tip apex, it provides high spatial resolution. While electromagnetic enhancement works in a nonselective way to enhance the signal from all the molecules immersed in the evanescent field, the chemical enhancement is related to the specific interaction where a chemical bonding between sample molecule and metal molecule results in the field enhancement. This enhancement mechanism for Raman scattered light involves the resonance Raman effect due to a dynamic charge transfer between the sample molecule and the metal molecule. Due to its specific-interaction nature, the spatial resolution in this interaction is even higher. Electromagnetic and chemical enhancement processes operate independently and the net effects are multiplicative. Further, the tip and the sample can also interact mechanically, if the metal molecules of the tip push against the sample molecules. This effect can be observed if the sample is pressurized, intentionally or unintentionally, by the tip. Unlike the isotropic hydraulic pressure usually studied in high-pressure Raman scattering, the pressure applied by a tip is unidirectional, and hence it can change the bond lengths uniaxially, resulting in modifications of the molecular vibrations.

Here in this paper, we investigate the tip effect in the NSOM studies of Buckminsterfullerene, carbon 60 (C_{60}), utilizing SERS, TERS, and their combination. The discovery of C_{60} has resulted in enormous research efforts to characterize and understand the basic properties of this interesting material. Some basic far-field Raman studies from large ensembles of C_{60} molecules were reported in early years,[21–24] however, with far-field technology, it was not possible to investigate this material any further with higher resolution. In Ref. 18, where the authors discussed the advantages of the TERS technique, an enhancement in the height-frequency Raman modes of the C_{60} sample was also reported. In the present study, the samples were prepared from commercially available C_{60} molecules, according to the experimental re-

quirements. The sample details are discussed along with individual experimental results. The samples were studied utilizing the near-field Raman scattering technique, and the enhancement of Raman scattering in SERS, TERS, and their combination was investigated. With a cagelike near-spherical hollow structure, C_{60} molecules are suitable for studying the effects of uniaxial pressure. The C_{60} molecules were pressurized by the tip in controlled manner, and the mechanical interaction between the tip and C_{60} molecule was studied quantitatively under uniaxial pressure, which, to the best of our knowledge, is reported here for the first time. The results were compared with theoretical calculations performed using the density functional theory (DFT). An anomalous shift in Raman frequency was explained by the possibility of polymerization of C_{60} molecules under a combined influence of radiation and tip pressure.

II. EXPERIMENTAL DETAILS

The experimental setup for Raman measurements consisted of an inverted confocal microscope, a frequency-doubled $Nd:YVO_4$ laser ($\lambda=532$ nm), and a spectrometer fitted with electronically cooled charge-coupled device (CCD) detector. The incident light was focused on the sample using a high-NA oil-immersion lens, and the scattered light was guided in the backscattering geometry through several optical elements, such as notch filter, pin holes, and narrow slits, to the spectrometer. For TERS measurements, an atomic force microscope (AFM) was added to the sample stage on the optical microscope. The tip was prepared by evaporating silver (thickness=30 nm) on the commercial silicon cantilever used in AFM. The tip apex was observed using scanning electron microscopy (SEM) and it was found that the size of the tip apex was about 30 nm. For the precise controls of the tip position and distance regulation in the near-field measurements, servo-controlled piezo scanning stages of the AFM were mounted directly on the inverted microscope. Photopolymerization of C_{60} under laser irradiation is quite a common problem. Therefore, it was necessary to carefully optimize the laser power density and the exposure time. All Raman spectra were measured for 60 s with 3.0 μW laser power. Raw data were calibrated and treated to remove the unwanted background signals, including the silicon and the glass structures, coming from the tip and the substrate, respectively.

III. RESULTS AND DISCUSSION

A. Surface-enhanced Raman scattering

The samples for SERS experiments were prepared by spincasting diluted C_{60}/toluene solution (1.0 μM) on a 4-nm-thick silver film evaporated on a glass cover slip. The silver layer also had a roughness of about 4 nm. C_{60} molecules were aggregated to about 5-nm-thick, 150-nm-large islands, as observed in the AFM topographic image of the sample. With this dispersion of aggregation, usually only one aggregation was under the focal spot during the SERS experiment. Figure 1 shows a SERS spectrum from this sample. Out of the ten well-known Raman active modes (two Ag modes, including one radial-breathing mode at 496 cm^{-1} and one tangential-stretching mode at 1470 cm^{-1}; and eight Hg modes) of C_{60} molecules,[25] eight (two Ag modes at 496 and 1470 cm^{-1} and six Hg modes at 273, 435, 710, 774, 1098, and 1425 cm^{-1}) were clearly observed even at such a weak excitation power used in our experiments. The positions of each Raman peak were found to be at the same energies as reported earlier.[25] The two Hg modes at 1250 and 1575 cm^{-1} were too weak to be identified under present experimental conditions. In fact, the mode at 1575 cm^{-1} was never observed in our experiments, therefore, we would consider only nine Raman modes in our discussion. A similar sample, except the silver layer, was also prepared for the far-field measurements for a comparison. As confirmed from the AFM image, this sample had similar average thickness, similar average cluster size, and similar C_{60} molecules concentration compared to the sample prepared for the SERS measurements. This sample showed no Raman signal (not shown in Fig. 1). This confirms that the sample thicknesses for the samples prepared in these experiments were too small to be observed under the far-field configuration; however, when enhanced by a silver layer, Raman signals could be observed. Thus we conclude that all the observed modes in Fig. 1 were enhanced by the silver film.

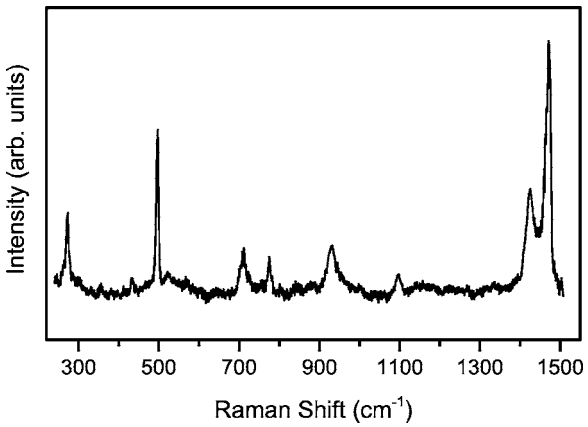

FIG. 1. SERS spectrum of C_{60} aggregates.

B. Tip-enhanced Raman Scattering

For the TERS experiments, the confined size of the nonpropagating photons was typically about 30 nm (same as the size of the tip apex). Therefore, for the best results, the sample should be of the thickness less than 30 nm. Much thinner samples are also not good, because in that case the Raman cross section is too small and hence it becomes difficult to experimentally observe the vibrational modes. Therefore, the samples for TERS measurement were prepared with thickness about 20~25 nm. This was done by dropping and evaporating C_{60}/toluene diluted solution (100 nM) on a glass cover slip, and then choosing an appropriate area from the dried sample. TERS spectra were measured from different parts of the sample by approaching a silver-coated silicon tip to the aggregates. The spectrum (a) in Fig. 2 shows one of such TERS spectra from a 150-nm-large and 20-nm-thick aggregate of C_{60} molecules. A corre-

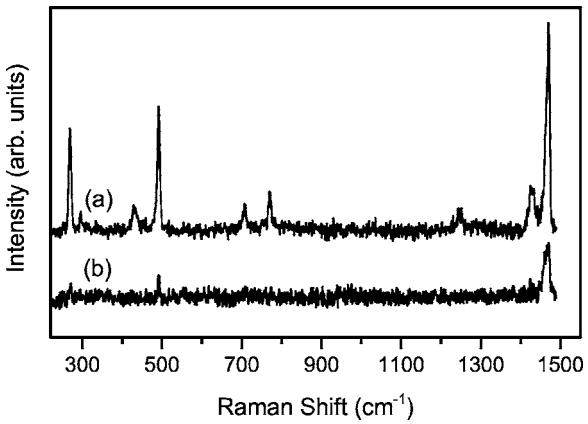

FIG. 2. (a) The near-field and (b) the far-field spectra of C_{60} aggregates.

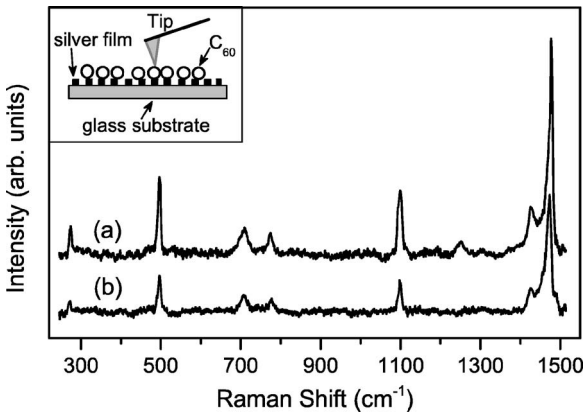

FIG. 3. (a) The gap-mode TERS and (b) the SERS spectra of C_{60} sample. The inset shows a schematic of the tip-sample combination for the gap-mode experiments.

sponding far-field spectrum, where the tip was taken off the sample, is presented by (b) in Fig. 2. All Raman modes were found to be enhanced in the TERS spectrum, compared to the far-field spectrum. The degrees of enhancement were different for different modes. Since this sample was thicker than that used in SERS experiments, unlike the far-field spectrum corresponding to the SERS experiment, a trace of the Ag modes at 496 and 1470 cm^{-1} could be observed in the far-field spectrum corresponding to the TERS experiment.

C. The gap-mode enhancement

In order to investigate a thinner sample with further improved enhancement, a combination of SERS and TERS techniques was employed for the first time. It has been theoretically evaluated in the past that if two metal nanoparticles, which are quite close to each other, are irradiated, then there is a huge field enhancement within the "gap" between them.[26,27] The strength of this enhancement depends on the particle size, the gap size, and the polarization direction. Hence, it can be predicted that if there is a sample in this gap, the Raman scattering from that sample would be strongly enhanced. The Raman spectra thus obtained can be called the "gap-mode" Raman spectra. When a tip, which is used in TERS experiments, approaches the metal-island film, which is used as the substrate in SERS experiments, then a similar condition is obtained, and a gap is created between the tip and the metal film. In order to investigate the gap-mode enhancement, a sample similar to the one used in SERS experiments was prepared, with the exception that the C_{60}/toluene solution was diluted to 100 nM. This sample was investigated in the close proximity of a metallic tip under the TERS configuration. A schematic of the sample-tip combination can be seen in the inset of Fig. 3. A 30-nm silver coated tip approached one of the C_{60} aggregates on 4-nm-thick silver film. It was estimated from the AFM image that there was only one C_{60} aggregate in the focal spot, and the aggregate was estimated to have about 10 000 molecules of C_{60}. However, the number of molecules near the tip apex (immersed in the evanescent field) was estimated to be only 3000. Thus, the gap-mode Raman spectra originated only from these 3000 molecules. The obtained gap-mode Raman spectrum is shown by (a) in Fig. 3. For comparison, a SERS spectrum from the same aggregate, when the tip was removed, is also presented by (b) in Fig. 3. Even though the number of molecules under the tip was much smaller than the number of molecules scattering in the SERS experiment, Fig. 3 shows that spectrum (a) is stronger compared to spectrum (b), which confirms a definite enhancement in the gap-mode configuration.

D. The tip-force effect

The tip-force effect on near-field Raman spectrum of C_{60} molecules was investigated, which is reported here for the first time. Far-field Raman scattering from C_{60} under isotropic hydraulic pressure has been reported in the past,[28] where a uniform pressure was applied in all directions. The shape of the molecule remains unchanged under a hydraulic pressure. However, when C_{60} molecules are squashed with the tip apex uniaxially, the shape of the molecules deform, the bond lengths change anisotropically and the molecules lose their degree of symmetry. Therefore, the spectral changes in pressure-dependent Raman spectra in the two cases differ from each other. As the symmetry of C_{60} molecule collapses with increasing uniaxial force, it is expected that the Hg modes get broadened. This is because the degeneracies of the five-fold degenerate Hg modes start losing, and the five modes start appearing individually at slightly different frequencies. This effectively broadens the whole Hg band. On the other hand, it is expected that the molecular vibrations for the nondegenerate radial-breathing Ag mode would be restricted by the external pressure, and hence the vibrational energy would be increased.

In order to justify our experimental results, the spectral changes in Raman modes of C_{60} molecules under uniaxial force were also estimated theoretically using the DFT calculations, derived from the molecular deformation caused by the tip force. The C_{60} molecules are composed of 60 carbon atoms, arranged in 12 pentagons and 20 hexagons, forming the shape of a soccer ball with a diameter of 0.71 nm. Each pentagon is surrounded by five hexagons. With this shape, there would be two independent configurations in which the

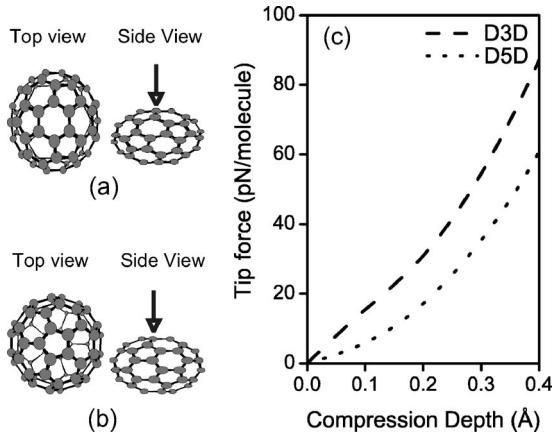

FIG. 4. Schematics of C_{60} molecule under uniaxial tip force in (a) D3D configuration and (b) in D5D configuration. (c) Theoretical plots showing the tip-force dependency on the compression depth of C_{60} molecule.

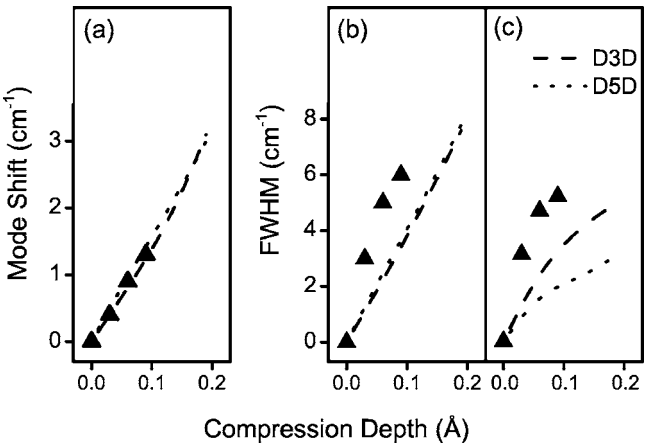

FIG. 5. Curves show the theoretical plots and the triangles show the experimental points for the relation between the compression depth and (a) shift in the frequency position of the Ag mode at 496 cm^{-1}, (b) FWHM for the Hg mode at 272 cm^{-1}, and (c) FWHM for the Hg mode at 710 cm^{-1}. The intrinsic width has been subtracted from the experimental points in (b) and (c).

C_{60} molecule could be deformed by the tip force, when the molecule is squashed between the tip and the substrate. One is the so-called D3D spheroidal deformation, where both apexes of the spheroid are formed by the hexagons, as shown in Fig. 4(a). The other is the D5D deformation, where the apexes are formed by the pentagons, as shown in Fig. 4(b). The geometrical structure of the C_{60} molecule was fully optimized at the B3LYP functional[29,30] using 6-31G(d) basis set,[31] which was then followed by calculations of the vibrational properties at the same level of the theory using the same basis set. The forces are calculated from a harmonic oscillation of the binding energy differences. The calculated geometry was a sphere shape (IH symmetry) which consisted of both the pentagons and the hexagons. Figure 4(c) shows the calculated relation between the tip force (which is the same as the van der Waals repulsive force accompanying the D3D and the D5D molecular deformation) and the change in the molecule dimension in the direction of the force, which we call the compression depth. As can be seen from Fig. 4(c), the elastic properties of C_{60} molecules differ slightly in the D3D and the D5D configurations. Since our experiments involve several C_{60} molecules, both D3D and D5D configurations are expected. Therefore, it is expected that the experimental results would compare with the average of the two theoretical calculations. The calculated vibrational frequencies had a constant factor difference with the experimental results. Multiplying the calculated vibrational frequencies by a constant scale factor of 0.985 provided a good fit between the calculated and the observed frequencies.[25] The curves in Figs. 5(a)–5(c) show the calculated relations between the compression depth and the shift in the Ag mode at 496 cm^{-1}, the full width at half maxima (FWHM) for the Hg mode at 272 cm^{-1}, and the FWHM for the Hg modes at 710 cm^{-1}, respectively. The dashed and the dotted lines in Fig. 5 correspond to the D3D and the D5D configurations, respectively.

The tip-force effect was experimentally investigated in two steps. In the first step, the SERS spectra were measured when the C_{60} molecules were pressurized by an uncoated silicon tip, and in the second step, the gap-mode spectra were measured when the C_{60} molecules were pressurized by a silver-coated silicon tip. In the first step, it is to be noted that the tip was not used for the near-field enhancement, rather it was simply used for applying a uniaxial force on the molecules. Therefore, it was neither necessary to have metal coating on the tip, nor was it necessary to have a tip with very sharp apex. In fact, if the size of the molecule aggregate under the focal spot is larger than the tip apex, then only a small part of the aggregate is pressurized by the tip, however, Raman scattering originates from the whole aggregate in the focal spot. Raman scattering from the pressurized molecules in such a situation is eclipsed by that from the unpressurized molecules. Therefore, in the SERS experiment, it is rather preferable to have a tip with an apex larger than the size of the aggregate. For this reason, a special tip was prepared by chopping off the tip apex of an AFM silicon cantilever, using the focused ion beam (FIB). The tip was prepared with a flat tip apex of 300 nm, which coincides with the focal spot size. The flatness of the FIB-modified tip was confirmed by observing the SEM image of the tip apex. The sample used was the same as that used in the previous experiment. A 100-nm-large C_{60} aggregate was placed at the center of the focal spot, and the FIB-modified tip was approached to the aggregate in order to apply a controlled uniaxial pressure on the aggregate. The force applied by the tip to the aggregate was sequentially increased from 0.7 nN to 8.7 nN (the corresponding force per molecule was estimated to range from about 0.8 pN to about 12 pN), and SERS spectra were measured under different forces, especially for the five-fold degenerated Hg modes at 273 and 710 cm^{-1}, and for the radial breathing Ag mode at 496 cm^{-1}. Considering the force per molecule and the displacement of carbon atoms in a molecule due to the tip force, the pressure on each molecule due to the tip force was also estimated for each value of force applied by the tip. Here, the isotropic force from the neighboring C_{60} molecules was neglected.

Figure 6 shows the SERS spectra for C_{60} molecules pressurized uniaxially under the varying tip force. The two Hg

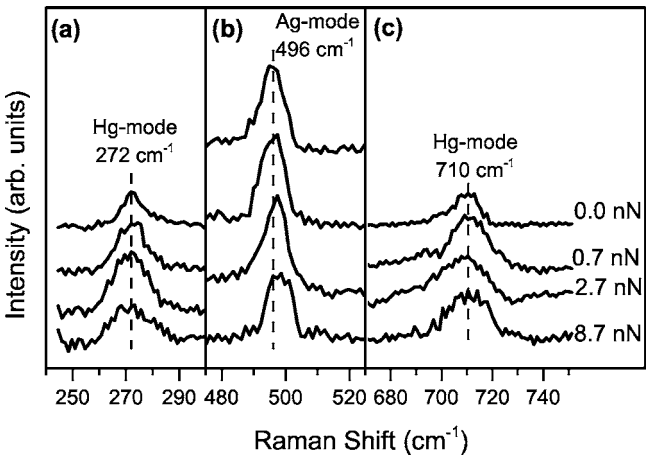

FIG. 6. SERS spectra under indicated uniaxial force applied by the tip. The Hg modes at 272 and 710 cm^{-1} in (a) and (c), respectively, show a broadening, while the Ag mode at 496 cm^{-1} in (b) shows a shift.

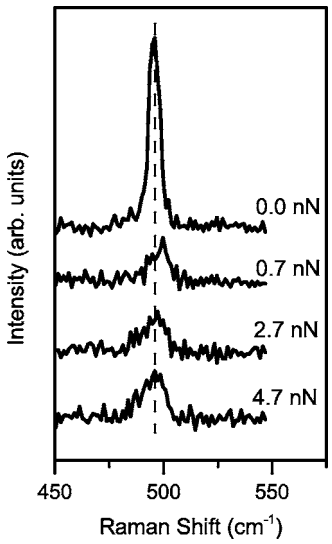

FIG. 7. The Ag mode at 496 cm^{-1} measured in the gap mode configuration under indicated uniaxial force applied by the tip. As the tip force increases, the mode first shifts to the higher frequency direction, and then toward the lower frequency direction.

modes at 273 and 710 cm^{-1} are shown in Figs. 6(a) and 6(c), respectively, and the Ag mode at 496 cm^{-1} is shown in Fig. 6(b). The intensity scales in Fig. 6 are arbitrarily adjusted for better viewing. The peak position of the Ag mode at 496 cm^{-1} shifts to higher frequency by about 1.5 cm^{-1} with increasing uniaxial pressure. The DFT calculation predicts a shift of 1.5 cm^{-1}, when the C_{60} molecule is uniaxially deformed to the diameter 7.00 Å from its original diameter of 7.10 Å. Figure 5(a) compared the theoretical plots with the experimental data (solid triangles in the figure) for the spectral shift in the Ag mode at 496 cm^{-1}, and the results are in excellent agreement.

Even though the Hg modes are weak in our experiments, a careful observation indicated a gradual increase in the FWHM of these modes, as expected. No frequency shifts were observed for these Hg modes. The experimental results for the two Hg modes were compared with the theoretical calculations, as shown by the solid triangles in Figs. 5(b) and 5(c), respectively. Since these modes are quite weak, there is a possibility of overestimation of the FWHM in experiments. Keeping that in mind, Figs. 5(b) and 5(c) show good agreement between theory and experiments.

In the next step, we investigated the tip-force effect by measuring the tip-enhanced gap-mode Raman spectra from uniaxially pressurized C_{60} molecules. The tip used here was the same as the one used in the TERS experiments (sharp tip, coated with 30-nm-silver layer). In order to reduce the background signal from the unpressurized molecules, the sample was prepared by dispersing a low concentrated C_{60} solution (0.1 μM) on a 4-nm-silver film. An AFM image indicated that the sample had C_{60} aggregates with a width of 40 nm and height of 5 nm. This aggregation contained about 1500 molecules. The tip was approached to one such aggregate and the gap-mode Raman spectra were measured at different tip forces. Since the scattering was collected from only a few molecules (about 1000 or less), the Raman modes were very weak. Even after gap-mode enhancement, out of the three modes in Fig. 6, only the radial-breathing Ag mode at 496 cm^{-1} was clearly observed. Obtained Raman spectra for this mode with increasing applied tip force are presented in Fig. 7. Since the number of C_{60} molecules under the tip was only about 1000, the force per molecule for a given tip force was much higher for this experiment, compared to the previous experiment. The molecules experienced much higher pressure for the same tip force. When the applied force was increased to 0.7 nN, the intensity of the mode drastically reduced and it shifted to the higher frequency side by 3 cm^{-1}. This behavior is expected from the DFT calculations. However, when the applied force was further increased to 2.7 nN and 4.7 nN, the mode shifted in the lower frequency direction by 1 and 3 cm^{-1}, respectively. This behavior is opposite of what is expected from the DFT calculations. In order to understand this low-frequency shift with increasing pressure, one needs to consider a different pressure-induced effect, independently responsible for a low-frequency shift. One possible reason is the polymerization of C_{60} molecules. It has been reported[32] that if a high pressure (about 1 GPa) is applied to C_{60} aggregates, the molecules tend to polymerize, and this phenomenon gives a low frequency shift to the radial breathing mode. Considering the tip apex to be 30 nm, assuming that there is no intermolecular gap for the molecules under the tip, and assuming a uniform pressure on all the molecules, we estimate that the uniaxial pressure on every molecule under the tip is about 7 MPa for the tip force of 4.7 nN. It looks difficult that the C_{60} molecules get polymerized at this pressure. However, if we consider the photo absorption at the probing wavelength (λ=532 nm) and consider photopolymerization at high pressure, then it is understandable to have polymerization of C_{60} molecules under a combination of probing light irradiation and a tip-applied pressure of 7 MPa. Here we recall that photopolymerization of C_{60} molecules was easily observed[33] when the probing laser power density was increased. Also, our assumptions in calculating the pressure due to tip force always underestimated the actual pressure, which means the

actual pressure on the C_{60} molecules could be much larger. The possible reasons could be that the actual tip end which touches the C_{60} molecules could be much smaller than 30 nm due to local curvatures, which is not observed in the SEM image; or that there are some intermolecular gaps between the C_{60} molecules under the tip. However, in order to confirm the phenomenon of polymerization under the combination of light irradiation and the tip force, the same sample was measured after removing the tip force, and it was found that the low-frequency shift persisted (with a decreased intensity) even after removing the pressure, which indicates a permanent change in the structure of the C_{60} aggregate under the tip. It is therefore concluded that the C_{60} molecules went under the polymerization process when they were pressurized under light irradiation.

IV. CONCLUSIONS

In conclusion, we have investigated the tip effects on C_{60} molecules, studied by NSOM Raman scattering. Enhancements of various Raman modes of C_{60} were observed in SERS and TERS experiments. A combination of SERS and TERS was employed for the first time to investigate gap-mode enhancement of Raman scattering for C_{60}. Apart from the electromagnetic and chemical effects, the mechanical effects were also investigated, where the C_{60} molecules were uniaxially pressurized by the tip. As predicted from the DFT calculations, a shift in the radial-breathing Ag mode and broadenings of the degenerate Hg modes were observed under increased pressure. Photopolymerization, which is a common feature of C_{60} molecules, was found to accelerate under high pressure.

ACKNOWLEDGMENTS

One of the authors (Y. I.) gratefully acknowledges financial support by the Grant-in-Aid for Scientific Research Grant No. 16360034 and the Ministry of Education, Science, Culture, Sports, and Technology Japan Grant No. 17034034.

*Corresponding author. Electronic address: verma@ap.eng.osaka-u.ac.jp

[1] D. P. Tsai, A. Othonos, M. Moskovits, and D. Uttamchandani, Appl. Phys. Lett. **64**, 1768 (1994).
[2] C. L. Jahncke, M. A. Paesler, and H. D. Hallen, Appl. Phys. Lett. **67**, 2483 (1995).
[3] H. D. Hallen and C. L. Jahncke, J. Raman Spectrosc. **34**, 655 (2003).
[4] R. E. Larsen and H. Metiu, J. Chem. Phys. **114**, 6851 (2001).
[5] A. V. Zayats and V. Sandoghdar, J. Microsc. **202**, 94 (2001).
[6] Y. Inouye and S. Kawata, Opt. Lett. **19**, 159 (1994).
[7] F. Festy, A. Demming, and D. Richards, Ultramicroscopy **100**, 437 (2004).
[8] A. L. Demming, F. Festy, and D. Richards, J. Chem. Phys. **122**, 184716 (2005).
[9] P. J. H. M. Fleischmann and A. J. McQuillan, Chem. Phys. Lett. **26**, 163 (1974).
[10] K. L. Akers, L. M. Cousins, and M. Moskovits, Chem. Phys. Lett. **190**, 614 (1992).
[11] S. J. Chase, W. S. Bacsa, M. G. Mitch, L. J. Pilione, and J. S. Lannin, Phys. Rev. B **46**, 7873 (1992).
[12] Z. Tian, B. Ren, and D. Wu, J. Phys. Chem. B **106**, 9463 (2002).
[13] Y. Inouye, N. Hayazawa, K. Hayashi, Z. Sekkat, and S. Kawata, Proc. SPIE **3791**, 40 (1999).
[14] N. Hayazawa, Y. Inouye, Z. Sekkat, and S. Kawata, Opt. Commun. **183**, 333 (2000).
[15] N. Hayazawa, Y. Inouye, Z. Sekkat, and S. Kawata, J. Chem. Phys. **117**, 1296 (2002).
[16] N. Hayazawa, Y. Inouye, Z. Sekkat, and S. Kawata, Chem. Phys. Lett. **335**, 369 (2001).
[17] H. Watanabe, Y. Ishida, N. Hayazawa, Y. Inouye, and S. Kawata, Phys. Rev. B **69**, 155418 (2004).
[18] R. M. Stoeckle, Y. D. Suh, V. Deckert, and R. Zenobi, Chem. Phys. Lett. **318**, 131 (2000).
[19] M. S. Anderson, Appl. Phys. Lett. **76**, 3130 (2000).
[20] A. Hartschuh, E. J. Sánchez, X. S. Xie, and L. Novotny, Phys. Rev. Lett. **90**, 095503 (2003).
[21] H. W. Kroto, J. R. Heath, S. C. O'Brien, R. F. Curl, and R. E. Smalley, Nature **318**, 162 (1985).
[22] W. Krätchmer, L. D. Lamb, K. Fostiropoulos, and D. R. Huffman, Nature **347**, 354 (1990).
[23] R. C. Haddon *et al.*, Nature **350**, 320 (1991).
[24] P. H. M. van Loosdrecht, P. J. M. van Bentum, and G. Meijer, Phys. Rev. Lett. **68**, 1176 (1992).
[25] D. S. Bethune, G. Meiger, W. C. Tang, H. J. Rosen, W. G. Golden, H. Seki, C. A. Brown, and M. S. de Vries, Chem. Phys. Lett. **179**, 181 (1991).
[26] J. Kottmann, O. Martin, D. Smith, and S. Schultz, Chem. Phys. Lett. **341**, 1 (2001).
[27] M. Futamata, Y. Maruyama, and M. Ishikawa, J. Phys. Chem. B **107**, 7607 (2003).
[28] S. H. Tolbert, A. P. Alivisatos, H. E. Lorenzana, M. B. Kruger, and R. Jeanloz, Chem. Phys. Lett. **188**, 163 (1992).
[29] A. D. Backe, J. Chem. Phys. **98**, 5648 (1993).
[30] C. Lee, W. Yang, and R. G. Parr, Phys. Rev. B **37**, 785 (1988).
[31] M. J. Frisch *et al.*, *Computer Code GAUSSIAN98 Revision A.9* (Gaussian Inc., Pittsburgh, PA, 1998).
[32] V. A. Davydov, L. S. Kashevarova, A. V. Rakhmanina, V. M. Senyavin, R. Ceolin, H. Szwarc, H. Allouchi, and V. Agafonov, Phys. Rev. B **61**, 11936 (2000).
[33] A. M. Rao *et al.*, Science **259**, 955 (1993).